

NASA TECHNICAL NOTE



NASA TN D-5568

2.1

NASA TN D-5568



LOAN COPY: RETURN TO  
AFWL (WLOL)  
KIRTLAND AFB, N MEX

# ALPHA-GAMMA ANGULAR CORRELATIONS IN THE REACTION CARBON-12( $\alpha, \alpha' \gamma_{4.433 \text{ MeV}}$ )

*by William M. Stewart, Norton Baron,  
Richard C. Braley, and Regis F. Leonard*

*Lewis Research Center  
Cleveland, Ohio*



0132361

1. Report No. NASA TN D-5568	2. Government Accession No.	3. Recipient's Catalog No.
4. Title and Subtitle ALPHA-GAMMA ANGULAR CORRELATIONS IN THE REACTION CARBON-12 ( $\alpha, \alpha'\gamma_{4.433 \text{ MeV}}$ )		5. Report Date November 1969
7. Author(s) William M. Stewart, Norton Baron, Richard C. Braley, and Regis F. Leonard		6. Performing Organization Code
9. Performing Organization Name and Address Lewis Research Center National Aeronautics and Space Administration Cleveland, Ohio 44135		8. Performing Organization Report No. E-5033
12. Sponsoring Agency Name and Address National Aeronautics and Space Administration Washington, D. C. 20546		10. Work Unit No. 129-02
		11. Contract or Grant No.
15. Supplementary Notes		13. Type of Report and Period Covered Technical Note
16. Abstract The angular correlation between inelastically scattered 41.2-MeV alpha particles and gamma rays emitted in the decay of the target nucleus has been measured for alpha scattering angles between $26^\circ$ and $95^\circ$ . The results are given in the form of A/B ratios and symmetry angles of the gamma ray distribution for a fixed alpha scattering angle. All measurements are in the plane of the original alpha scattering. In an auxiliary experiment the cross sections for both the elastic and inelastic ( $Q = -4.433 \text{ MeV}$ ) scattering have also been measured over the angular range $2.5^\circ \leq \theta_\alpha \leq 170^\circ$ . Neither the cross sections nor the correlations are correctly predicted by theory.		14. Sponsoring Agency Code
17. Key Words (Suggested by Author(s)) $^{12}\text{C} (\alpha, \alpha'\gamma_{4.433 \text{ MeV}})$	18. Distribution Statement Unclassified - unlimited	
19. Security Classif. (of this report) Unclassified	20. Security Classif. (of this page) Unclassified	21. No. of Pages 30
		22. Price* \$3.00

\*For sale by the Clearinghouse for Federal Scientific and Technical Information  
Springfield, Virginia 22151

# ALPHA-GAMMA ANGULAR CORRELATIONS IN THE REACTION

CARBON-12 ( $\alpha, \alpha'\gamma_{4.433 \text{ MeV}}$ )

by William M. Stewart, Norton Baron, Richard C. Braley,  
and Regis F. Leonard

Lewis Research Center

## SUMMARY

The angular correlation between inelastically scattered 41.2-MeV alpha particles and gamma rays emitted in the decay of the target nucleus has been measured for alpha scattering angles between  $26^\circ$  and  $95^\circ$ . The results are given in the form of symmetry angles of the gamma-ray distribution for a fixed alpha scattering angle and the ratio of isotropic to anisotropic components. All measurements are in the plane of the original alpha scattering. In an auxiliary experiment the cross sections for both the elastic and inelastic ( $Q = -4.433 \text{ MeV}$ ) scattering have also been measured over the angular range  $2.5^\circ \leq \theta_\alpha \leq 170^\circ$ . The results of both the cross section and angular correlation measurements are compared with calculations based on the optical model and distorted-wave Born approximation. Neither these nor coupled-channels calculations are able to predict both the cross sections and angular correlations accurately.

## INTRODUCTION

The angular correlation between inelastically scattered alpha particles and the gamma rays emitted in the subsequent decay of the excited nuclear state is a quantity that should be sensitive to the details of any calculation that attempts to describe the scattering process. This was shown in earlier work (refs. 1 to 3), where considerable deviation was observed from the predictions of the simple theories (plane-wave Born approximation and adiabatic approximation; refs. 4 and 5) which are usually able to predict the main features of differential cross sections for elastic and inelastic scattering. In particular, the correlation pattern exhibited rapid reverse rotations rather than the slow forward ones predicted. At forward scattering angles this behavior could be qualitatively explained using the Wills-Cramer (ref. 6) or Inglis (ref. 7) models. In addition

a quantitative description could be obtained using a distorted-wave Born approximation (DWBA) calculation. The present experiment was undertaken in order to determine whether this rapid reverse rotation persists at alpha-scattering angles larger than those measured in reference 1. Such information should be helpful in obtaining an understanding of the scattering of the alpha particles from carbon-12 and also in understanding the structure of carbon-12 (if calculations become available which are structurally dependent). In the present experiment the angular correlation between inelastically scattered alpha particles, which produce excitation of the 4.433-MeV state of carbon-12, and the 4.433-MeV gamma, which is emitted in the decay of that state, was measured. The use of a multiple detector arrangement resulted in reduced data-taking times which permitted both verification of the results of reference 1 and their extension to alpha-scattering angles of approximately  $95^\circ$ .

In order to compliment this increased angular range of the correlation data, elastic and inelastic cross sections were measured over an extended angular range. Using a four-detector arrangement, cross sections were measured from  $16^\circ$  to  $170^\circ$  in increments of  $1^\circ$  or  $2^\circ$ . In addition, using a single detector, measurements were made at forward scattering angles as small as  $2.5^\circ$ . In the course of these measurements, cross sections were also obtained for the 7.65- and 9.61-MeV levels.

The data obtained have been compared with DWBA predictions using both the optical potential presented in reference 1 and using new optical potentials derived to fit the more extensive cross-section data reported here. A number of coupled-channels calculations were also done in an attempt to obtain better descriptions of both cross-section and correlation data.

## SYMBOLS

- A magnitude of isotropic component of alpha-gamma correlation function
- $a_i$  diffuseness of form factor for imaginary part of optical model potential
- $a_o$  diffuseness of form factor for real part of optical model potential
- B magnitude of anisotropic component of alpha-gamma correlation function
- Q excess of final kinetic energy over initial kinetic energy in nuclear reaction
- $r_i$  radius of form factor for imaginary part of optical model potential
- $r_o$  radius of form factor for real part of optical model potential
- V strength of real part of optical potential
- W strength of imaginary part of optical potential

$W(\theta_\gamma)$	correlation pattern in reaction plane
$\theta_0$	symmetry angle of alpha-gamma correlation function
$\theta_\alpha$	scattering angle for alpha particles in center-of-mass system
$\theta_\gamma$	angle of emission of gamma ray, relative to incident beam direction
$d_\sigma/d\Omega$	differential cross section
$\chi^2$	a measure of statistical goodness of fit

## EXPERIMENTAL ARRANGEMENT

### Angular Correlation

The system for handling the 41.2-MeV alpha-particle beam of the NASA 1.5-meter cyclotron has been described in detail previously (ref. 8). Neither the slit system, the beam catcher, nor the shielding system have been changed. An overall diagram of the experiment is shown in figure 1.

Gamma-ray detection was provided by a 7.62- by 7.62-centimeter sodium iodide (Tl) crystal 12.7 centimeters from the target, so that the detector face subtended a full angle of about  $35^\circ$ , and covered about 2.2 percent of the total sphere. The gamma spectrum seen on bombardment of the carbon-12 target is shown in figure 2.

For the present experiment, an array of 13 lithium-drifted-silicon detectors was used for alpha-particle detection. The full angular resolution of the individual alpha detectors was  $1^\circ$ . Spacing between detectors was  $4^\circ$ . An overall block diagram of the electronic system is shown in figure 3. The individual alpha-particle signals enter the 16-channel router where they are amplified and added. The outputs of the router, in turn, feed a timing circuit and an energy analysis circuit. The linear signals are analyzed and stored in one of the sixteen 256-channel subgroups of the multichannel pulse-height analyzer, provided they occur in time coincidence with a gamma of the proper energy, as determined by a single-channel pulse-height analyzer. The coincidence circuit for the experiment was a standard parallel fast-slow arrangement with a resolving time of 40 nanoseconds, which is smaller than the time (100 nsec) between beam pulses of the cyclotron.

A more detailed diagram of the 16-channel router is shown in figure 4. Each alpha particle signal has its own amplifier system, which produces two outputs. One of these, the output of the first stage, is unshaped and is used to provide timing for the alpha side of the coincidence circuit. The other output of the channel amplification system has been shaped so that the best possible energy resolution may be obtained after mixing. The remainder of the router consists of two operational amplifiers into which the timing

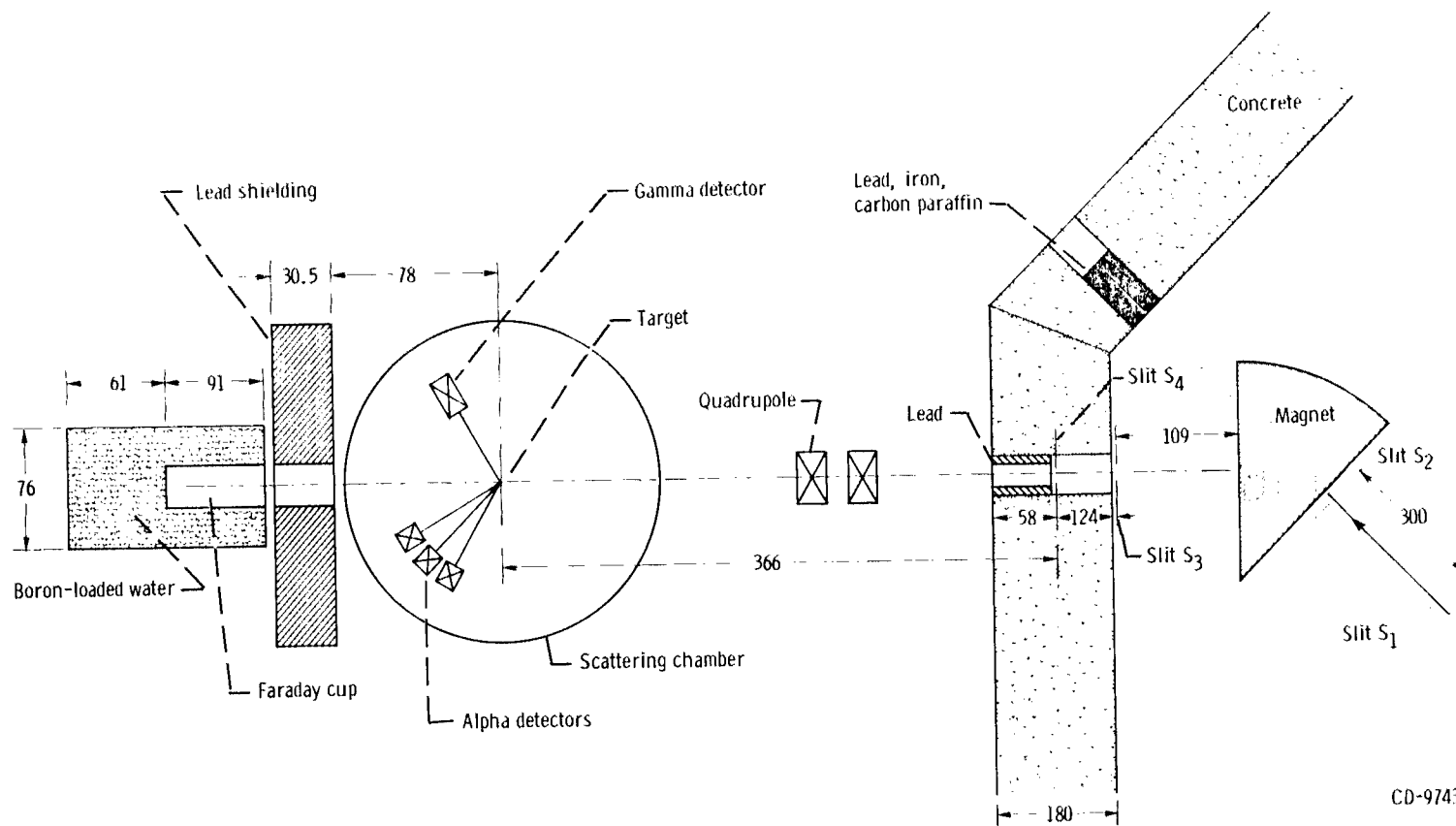


Figure 1. - Schematic diagram of scattering system. (All dimensions are in centimeters.)

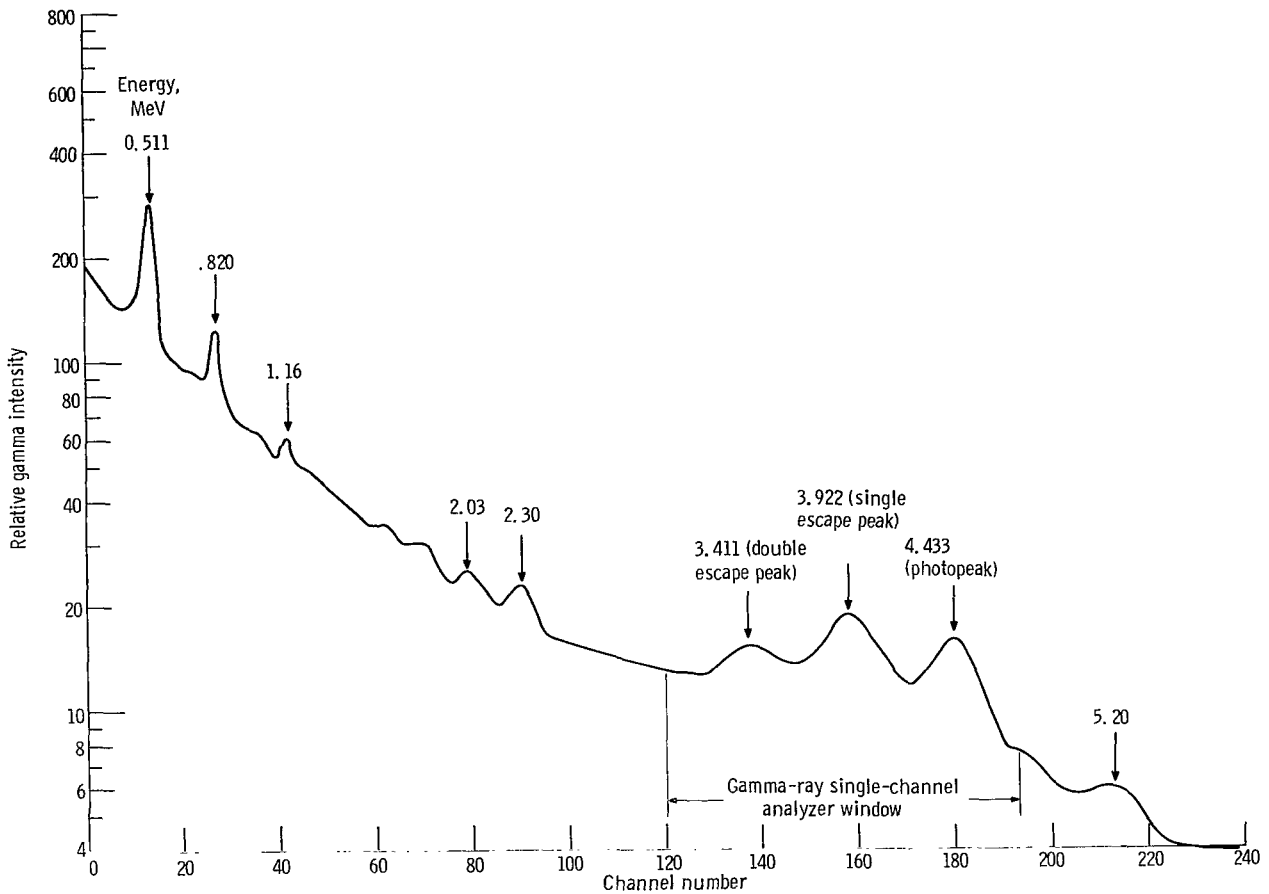


Figure 2. - Gamma ray spectrum resulting from bombardment of carbon-12 with 41-MeV alpha particles.

and energy signals are mixed and the logic that is needed to insure that the signals are stored in the proper subgroup of the multichannel analyzer. Principally, this logic consists of a series of gates which allow a signal to be stored in the analyzer only if (1) no pulse has occurred simultaneously in another channel, (2) the analyzer is prepared to analyze a pulse, and (3) there has been an output from the slow coincidence circuit (indicating that a gamma signal has occurred simultaneously and that both the alpha and gamma were of the energies of interest). If all of these conditions are satisfied, a gate pulse is transmitted to the analyzer's coincidence input, a routing pulse is generated, and a "live count" output is generated. The ratio of the number of live counts to the total number of coincidences then yields the dead time correction, that is, the percentage of counts that are lost either because the analyzer is busy or because pulses have occurred simultaneously in two alpha detectors.

The target for these measurements was a 1 milligram per square centimeter natural carbon foil.

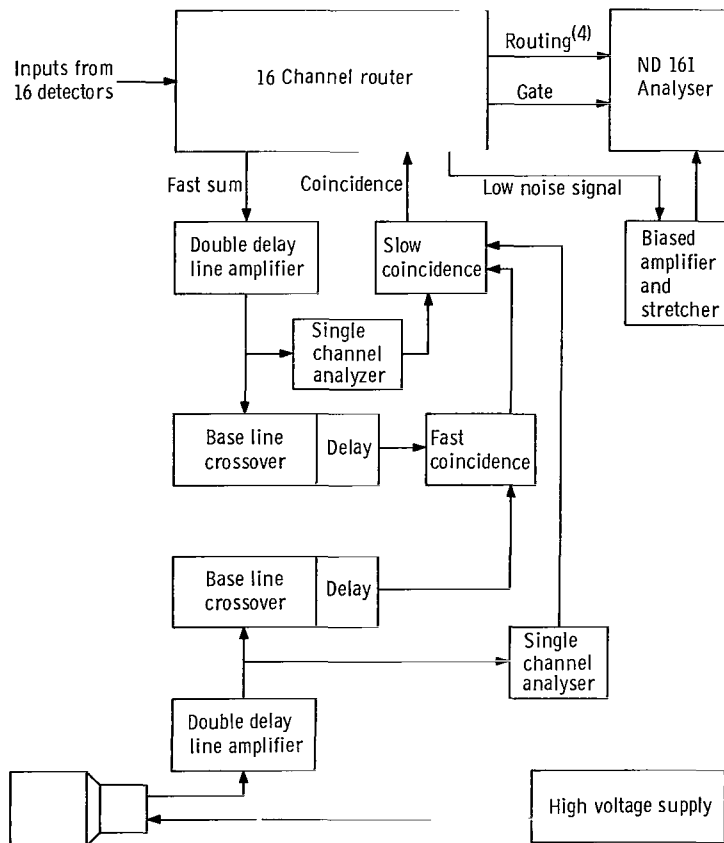


Figure 3. - Typical multidetector coincidence arrangement using 16-channel router.

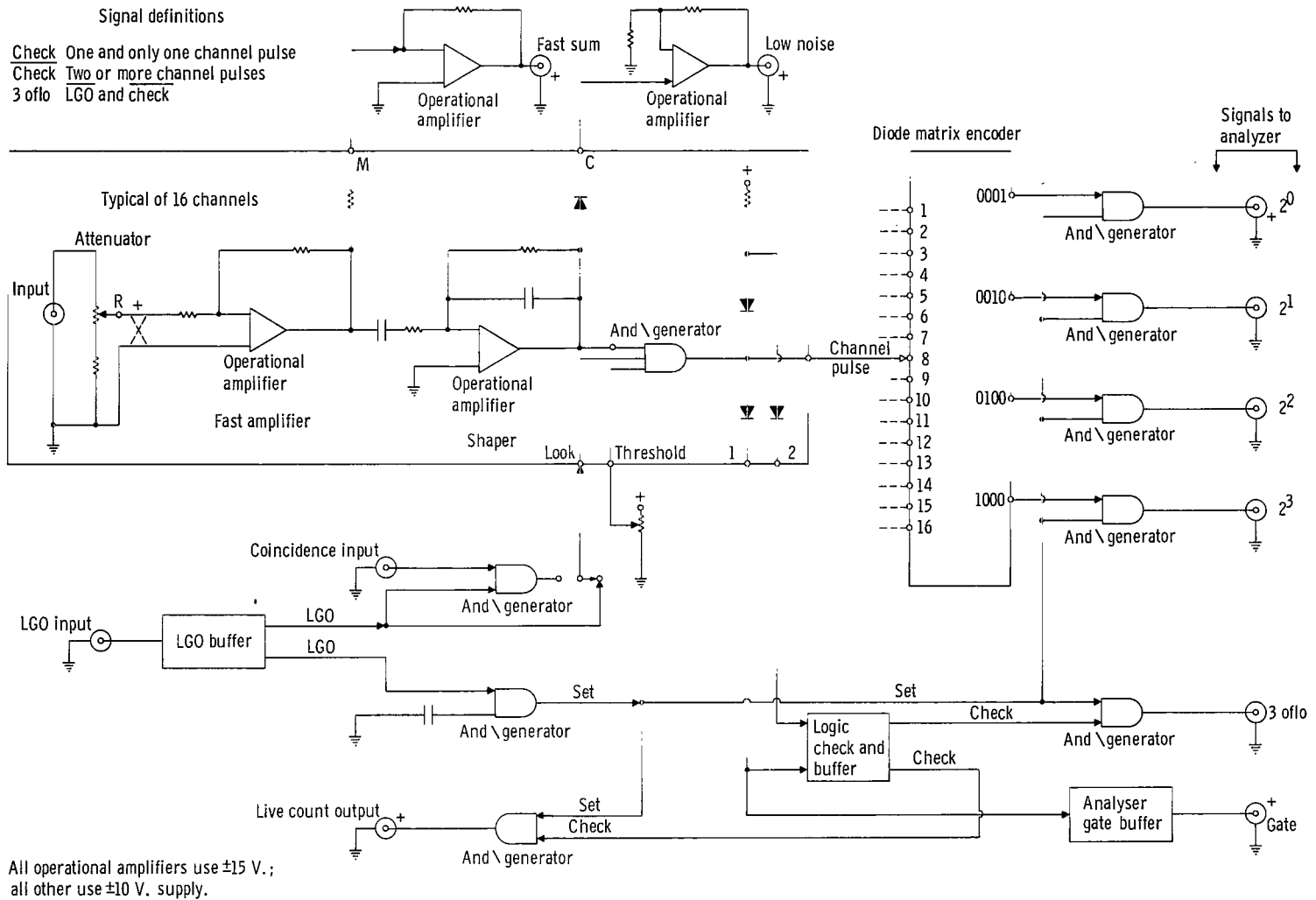


Figure 4. - Logic schematic for 16-channel routing system.

## Cross Section Measurements

Cross sections have been measured for elastic scattering of 41.2-MeV alpha particles and for inelastic scattering with excitation of the 4.433-, 7.65-, and 9.61-MeV states of carbon-12. For angles greater than  $16^\circ$ , the experimental arrangement was identical to that previously described for this type of experiment (ref. 9). A four-detector mount was used with each detector having a full angular resolution of  $0.5^\circ$ . The target used was a 270-microgram-per-square-centimeter natural carbon foil. For most of the experiment the energy resolution was about 250 keV.

For the extreme forward angles a single detector was used at the largest radius (750 mm) permitted by the scattering chamber. At this radius the detector slits employed (2 by 6 mm) subtended an angle of  $0.07^\circ$  in the horizontal plane. At the foremost angle examined ( $2^\circ$ ) the vertical height of the slit increased the angular resolution by only  $0.01^\circ$ , assuming a point source on the target and parallel beam. For the worst possible geometric errors (a  $0.50^\circ$  vertical divergence in the incident beam and a 6-mm high beam spot) all particles that enter the detector have still been scattered through angles between  $1.93^\circ$  and  $2.28^\circ$  when the detector is set at  $2^\circ$ . Corrections for right-left errors in the incident beam direction were made by scattering on both sides of the beam. This resulted in a  $0.17^\circ$  correction to the alpha-scattering angle.

The cross sections (in mb/sr) and their statistical errors are listed in table I. In addition there is a systematic error of approximately 5 to 10 percent in the cross sections for elastic scattering and scattering to the first excited state due to uncertainties in target thickness. For the 7.65- and 9.61-MeV states this additional error is probably 10 to 15 percent because of the uncertainties in separating the peaks from the background which exists at the lower alpha energies where these peaks appear.

## DATA-TAKING PROCEDURES AND DATA REDUCTION FOR ANGULAR CORRELATION MEASUREMENTS

Data were taken over the angular range  $45^\circ \leq \theta_\gamma \leq 135^\circ$  and  $26^\circ \leq \theta_\alpha \leq 95^\circ$ . Measurements were made in  $10^\circ$  intervals of the gamma angle and in  $2^\circ$  intervals in the alpha-scattering angle. Typical alpha-particle energy spectra with and without a coincidence requirement are shown in figure 5. The size of the elastic scattering peak in the coincidence spectrum determines the number of random coincidences that occur, as explained in reference 8. The incident beam current for most runs was between 10 and 15 nanoamperes, which resulted in a true-to-chance ratio between 1:3 and 3:1.

Coincidence yields were normalized from run to run by using the output of a monitor counter which was fixed at a  $35^\circ$  angle below the beam line in the forward direction.

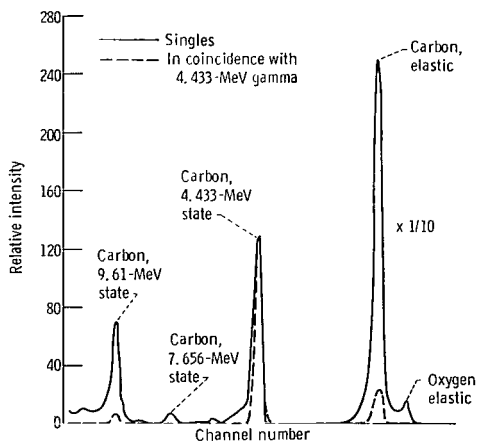


Figure 5. - Energy spectra of scattered alpha particles. Laboratory alpha particle scattering angle,  $32^\circ$ ; gamma-ray angle of emission,  $120^\circ$ .

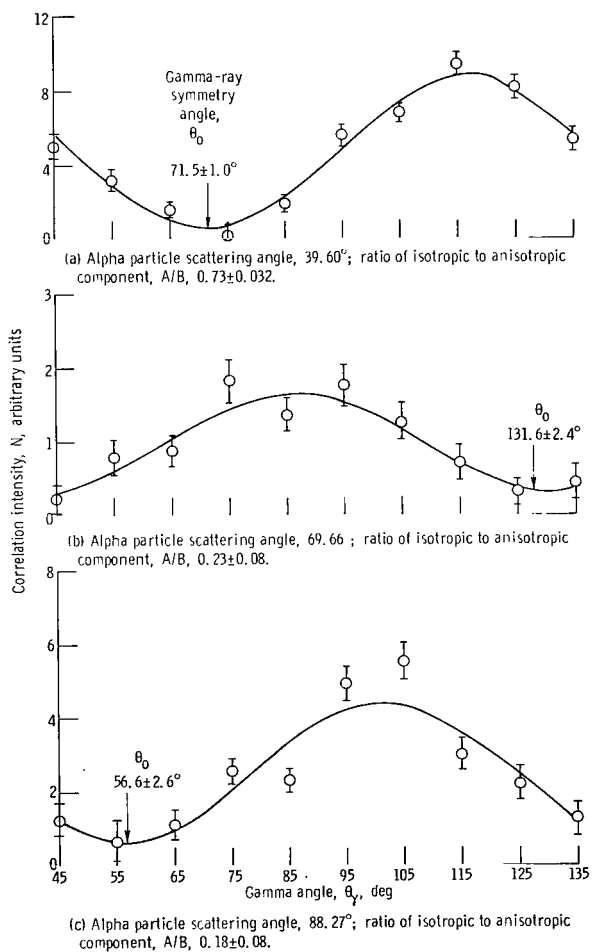


Figure 6. - Typical correlation patterns observed in reaction carbon-12 ( $\alpha, \alpha'\gamma$ ). Lines are least squares fits of the function  $W = A + B \sin^2 2(\theta_\gamma - \theta_0)$ . The  $A/B$  values given are without finite geometry connections.

Several gamma-ray correlation patterns are shown in figure 6. The line indicated on these figures results from a least squares fit to the data using the known (ref. 8) form of the correlation function in the reaction plane

$$W(\theta_\gamma) = A + B \sin^2 2(\theta_\gamma - \theta_0)$$

In addition, the data were corrected for the finite solid angle of the gamma detector using the method outlined in references 6 and 3. This correction is not shown in figure 6. The measured symmetry angles and geometry-corrected ratios  $A/B$  are listed in table II. They are also shown together with the earlier data of Hendrie (ref. 2) in figures 7. Both the symmetry angles and  $A/B$  ratios exhibit reasonably good agreement with Hendrie's measurements where there is overlap.

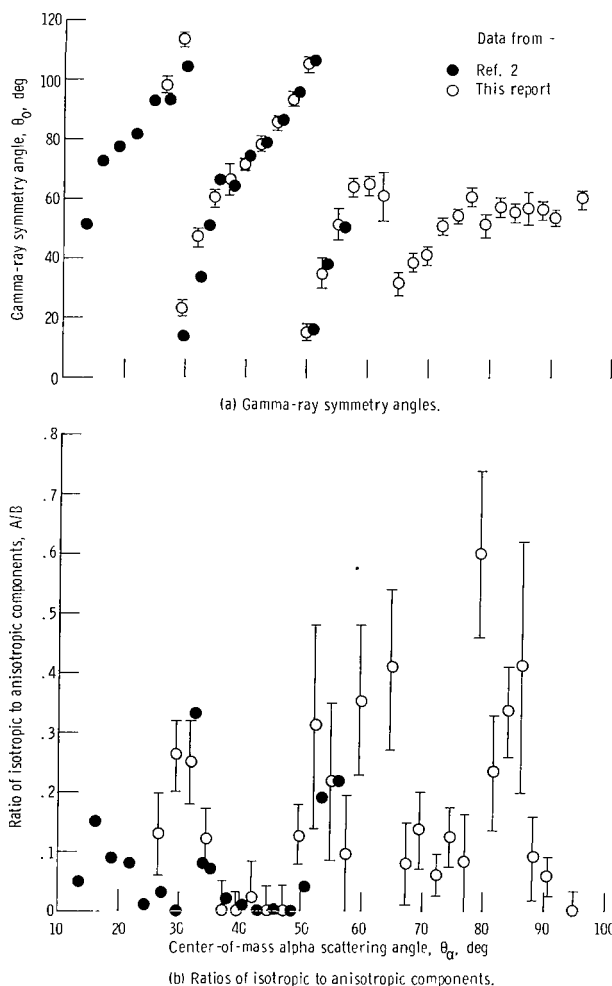


Figure 7. - Experimental results of reaction carbon-12 ( $\alpha, \gamma$ ) at scattering energy of 41.2 MeV.

## COMPARISONS WITH THEORY

### Optical Model and Distorted Wave Born Calculations

Conventional optical model calculations and distorted-wave Born calculations (DWBA) have been carried out using five different optical potentials. These are listed in table III.

The actual calculations were carried out using the computer programs SCAT4 (ref. 10) and DRC (ref. 11).

The first potential tested was that published by McDaniels et al. (ref. 1), and it is listed as potential A in table III. This potential was derived to fit only the forward

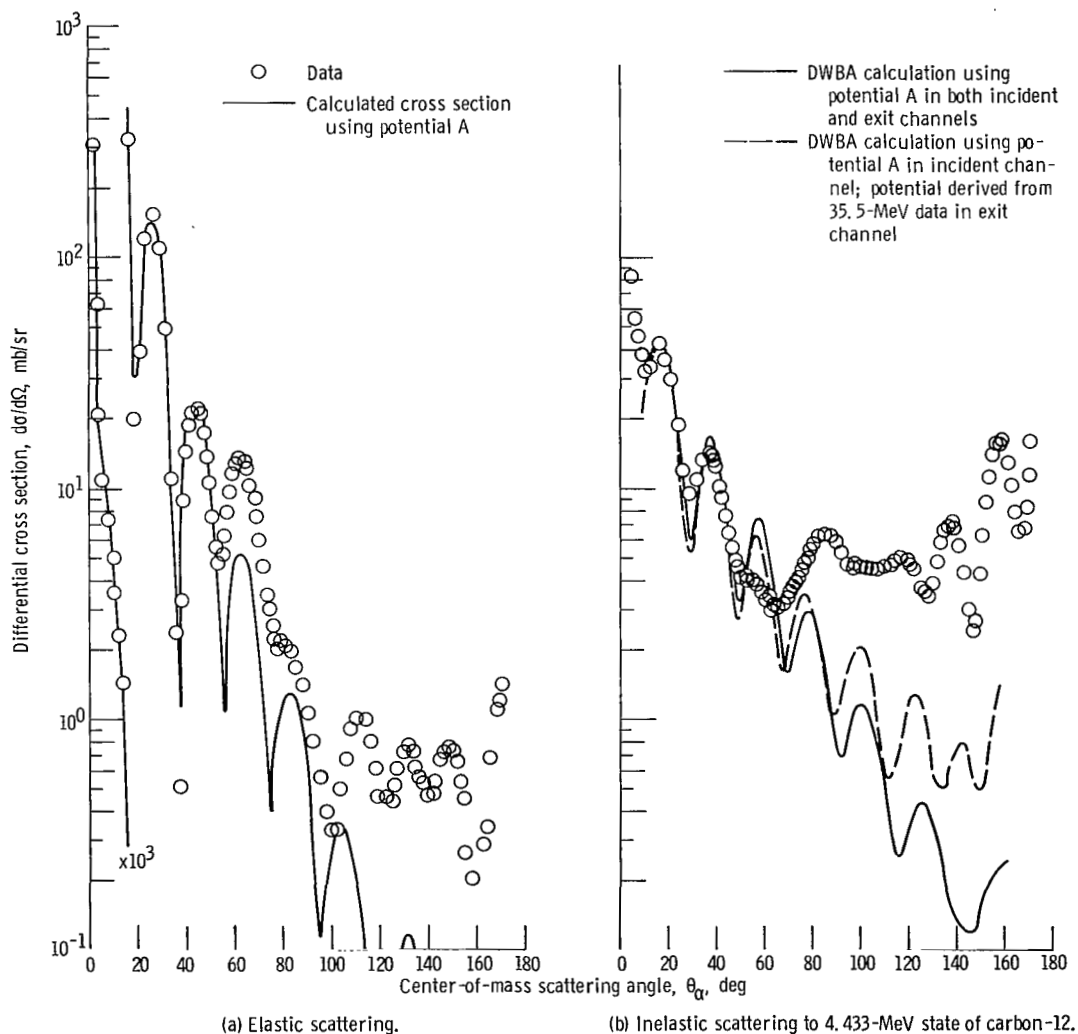


Figure 8. - Cross section for scattering of 41.2-MeV alpha particles from carbon-12. Four-parameter optical potential A.

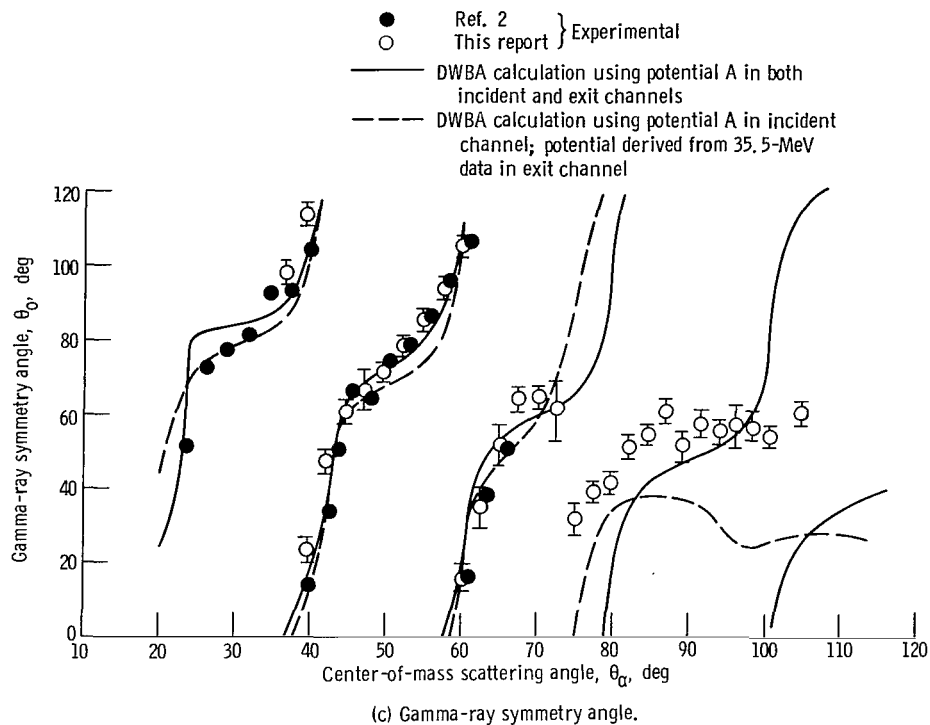


Figure 8. - Concluded.

angle ( $\theta_{\alpha} \leq 60^{\circ}$ ) data and gave reasonably good fits to all of the data (elastic cross sections, inelastic cross sections, and correlation data) in that angular range. This is shown in figure 8. Comparison with the newly acquired data, however, indicates that at larger angles there is considerable divergence between the theoretical prediction and the experimental data. This is particularly noticeable in the inelastic cross section and the correlation data. Experimentally, the inelastic cross section rises at back angles, while the calculated cross section continues to fall. As for the correlation data, this potential predicts a continuation of the rotations present at the more forward angles, but the symmetry angle in fact ceases rotating beyond about  $60^{\circ}$ .

The first attempt to improve the theoretical predictions consisted of searching for a new potential using as a starting point the parameters of McDaniels et al. (ref. 1) and then minimizing  $\chi^2$  as calculated over the entire angular range of available data. The first such searches using all of the data indicated that data at deep minima in the elastic cross section were contributing disproportionately to the value of  $\chi^2$ . Inasmuch as these are the data in which the least experimental confidence is justified (because of the steepness of descent to the minima and the effects of finite angular resolution), the data at  $18.80^{\circ}$ ,  $37.18^{\circ}$ ,  $53.81^{\circ}$ ,  $99.35^{\circ}$ ,  $101.46^{\circ}$ , and  $158.35^{\circ}$  were not included in the searches that are reported here. Potential B (table III) which resulted from using McDaniels parameters as a starting point was used to calculate the elastic and inelastic

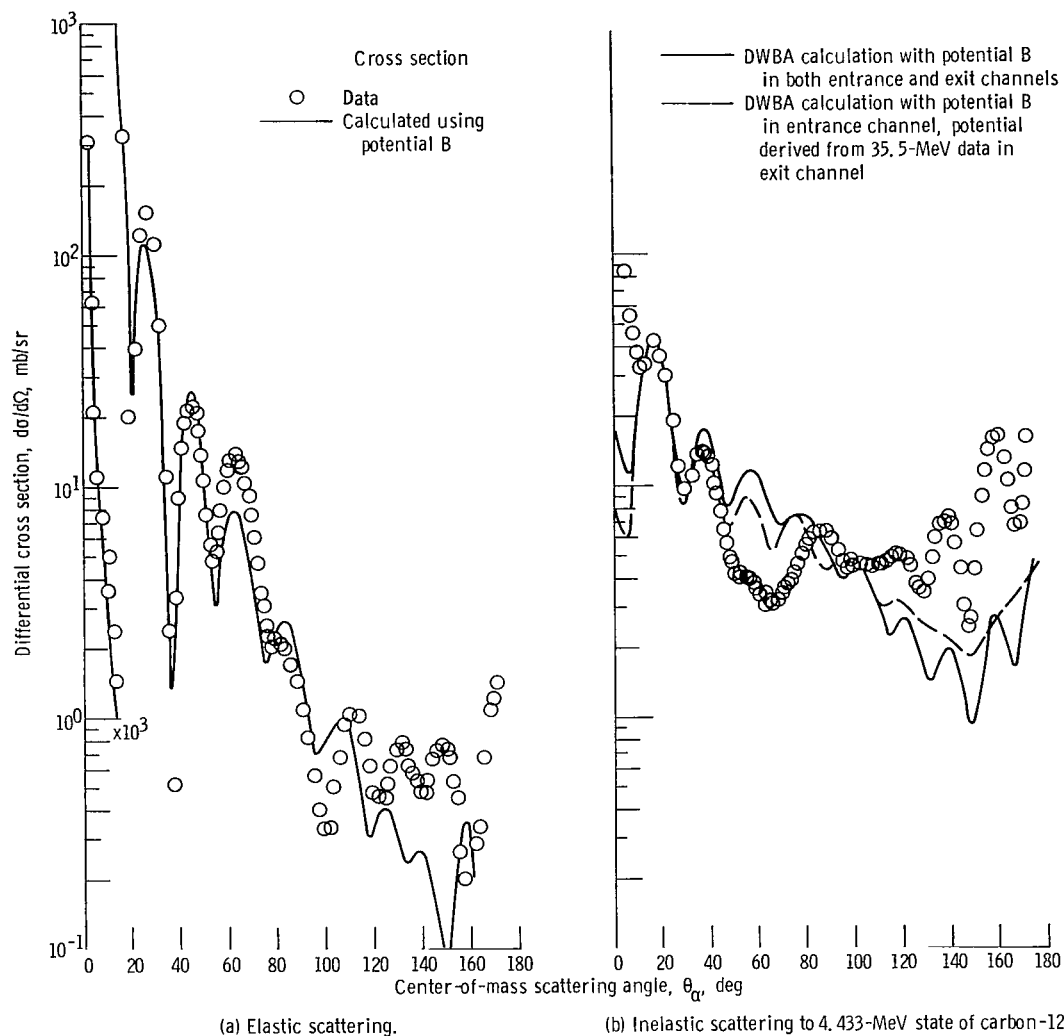
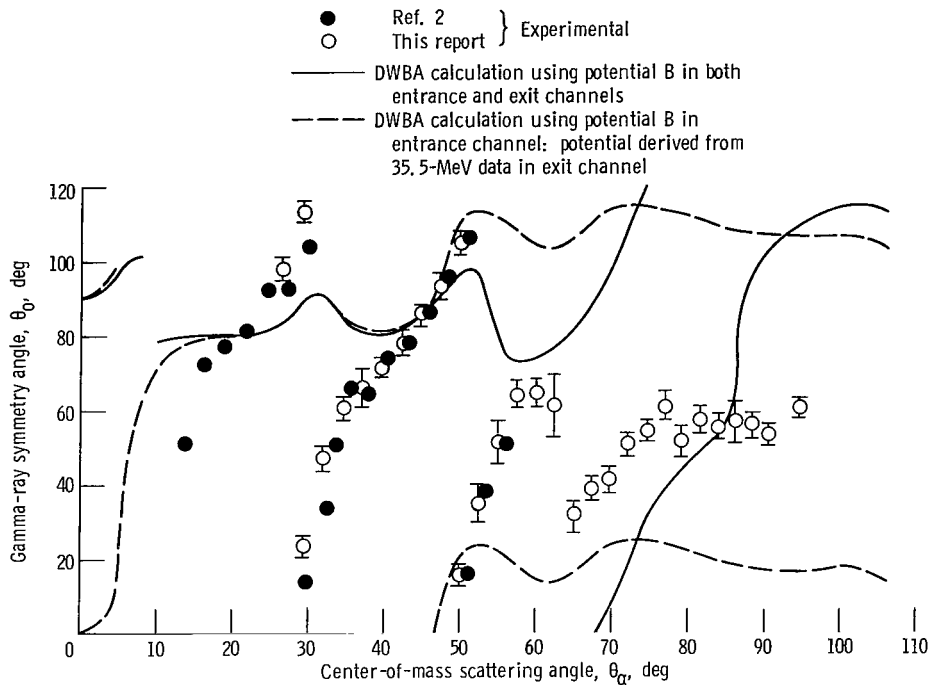


Figure 9. - Cross section for scattering of 41.2-MeV alpha particles from carbon-12. Four-parameter optical potential B.

cross sections as well as the symmetry angle of the angular correlation pattern shown in figure 9. It is clear that this process has improved the fit to the elastic data considerably ( $\chi^2$  is reduced by more than a factor of two), especially at the back angles. With the inelastic cross section a similar situation exists, and, although the fit is still rather poor, the overall magnitude at back angles is much closer to the experimental data than that predicted by the original potential of McDaniels et al. (ref. 1). The quality of fit to the correlation data, however, has deteriorated considerably compared with the original calculation.

As a result of this deterioration, a new potential was sought. For this purpose, a series of searches was conducted in which the nuclear radius constant was held fixed at values between 1.2 and 2.0 femtometers, while  $V$ ,  $W$ , and  $a$  were optimized. The

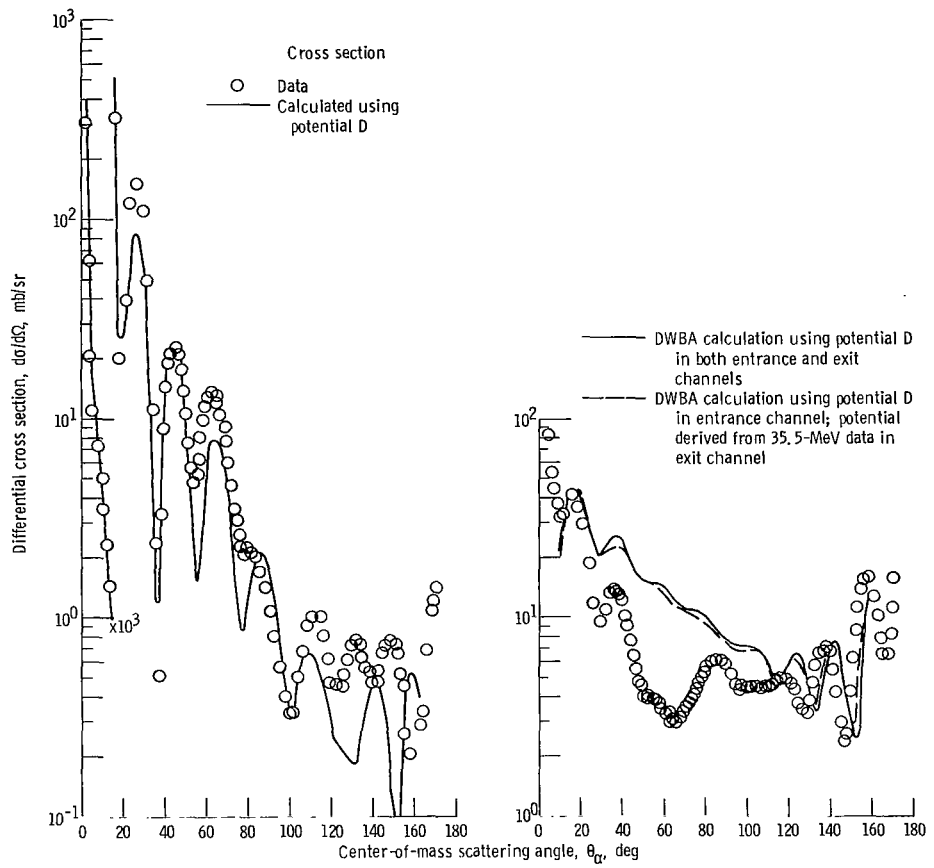


(c) Gamma-ray symmetry angle.

Figure 9. - Concluded.

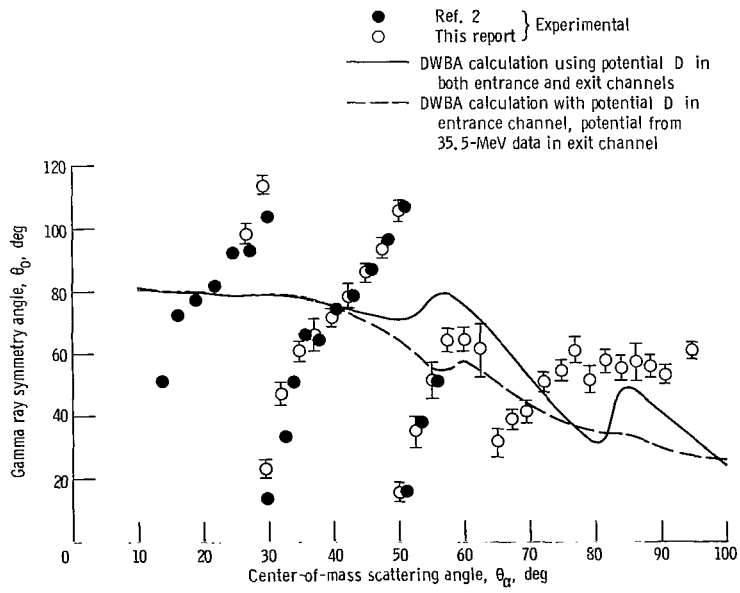
final values, which resulted from this procedure, were then used as the starting values in a series of searches in which all four potential parameters were allowed to vary. Of the parameters obtained in this way, only two sets gave good fits to the elastic scattering cross section. These two are listed in table III as potentials C and D. The first of these is virtually identical to that which resulted when McDaniels' potential was used as a starting value. Potential D gives nearly as good a fit to the elastic cross section ( $\chi^2$  is 14 percent larger than that obtained using potentials B and C). However, the inelastic fit is slightly poorer than potential C, while the correlation pattern calculated using potential D bears absolutely no resemblance to the experimental data. This is shown in figure 10.

Another series of searches similar to that just described was also conducted in which the depth of the nuclear potential was fixed at 150 and 200 MeV while the nuclear radius was varied in steps of 0.2 femtometer between 1.0 and 2.0 femtometer and the imaginary strength and diffuseness were automatically optimized. The two best of these 10 results were then used as starting values in searches in which all four parameters were allowed to vary. One such result is listed in table III as potential E. The comparison of this prediction with cross section and correlation data is not shown, inasmuch as it represents no great improvement over the potentials for which these are shown.



(a) Elastic scattering.

(b) Inelastic scattering to 4.433-MeV state of carbon-12.



(c) Gamma-ray symmetry angle.

Figure 10. - Cross section for scattering of 41.2-MeV alpha particles from carbon-12. Four-parameter optical potential D.

The last potential listed in table III, potential F, allowed the real and imaginary parts of the optical potential to have different radii and diffusenesses. The parameters listed there result from starting from the best four-parameter potential (potential C) and allowing all six parameters to vary. The results are shown in figure 11. The values listed in table III gave a minimum in  $\chi^2$  which was only 5 percent lower than could be obtained with a four-parameter potential. The inelastic cross section is fit no better than with potentials B and C, and there is little improvement in the fit to the correlation data. Thus it appears that very little is gained by using a six-parameter potential.

The final attempt to improve the optical model calculations consisted of changing the optical potential employed in the exit channel of the DWBA calculation. Because of the high negative Q-value, outgoing alpha particles have a center-of-mass energy of only

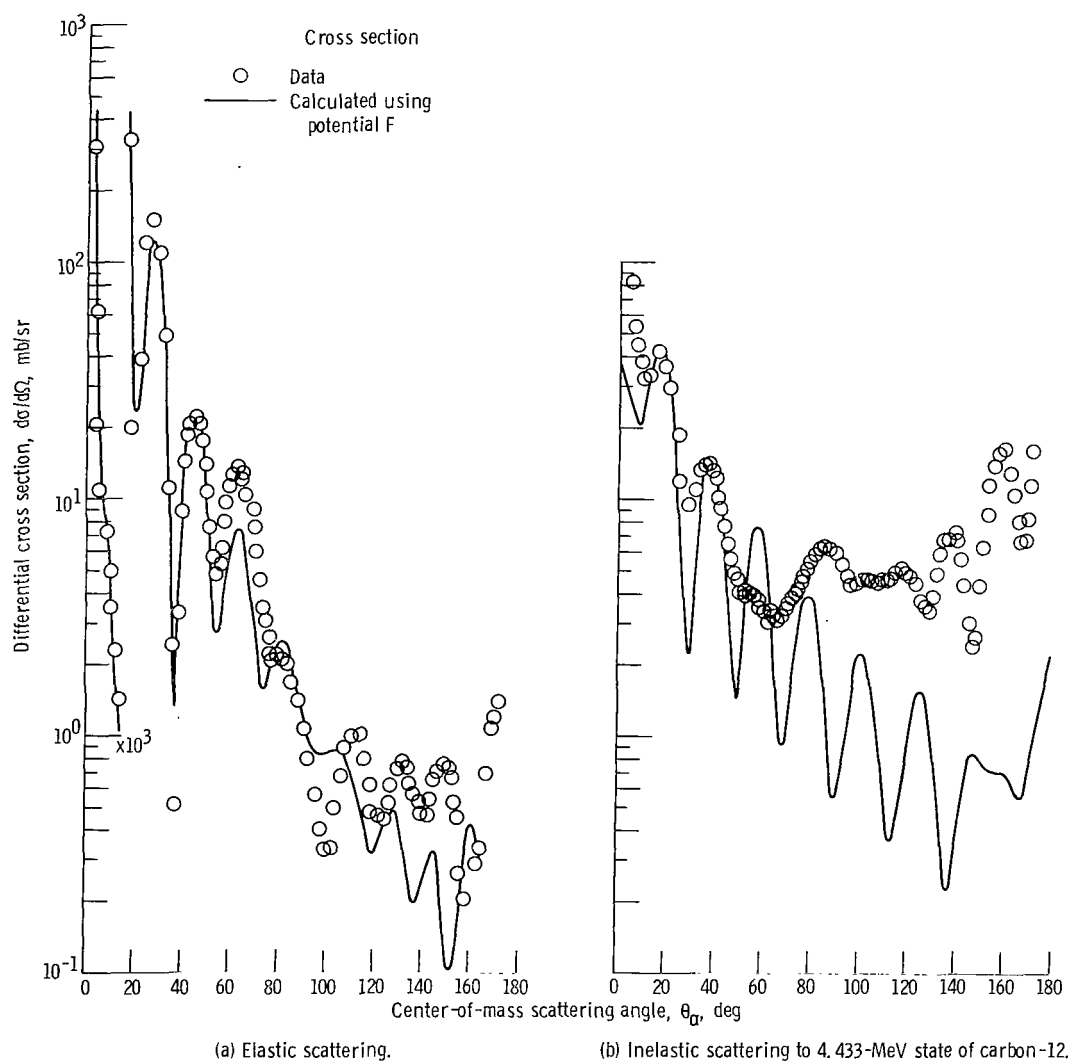


Figure 11. - Cross section for scattering of 41.2-MeV alpha particles from carbon-12. Six-parameter optical potential F.

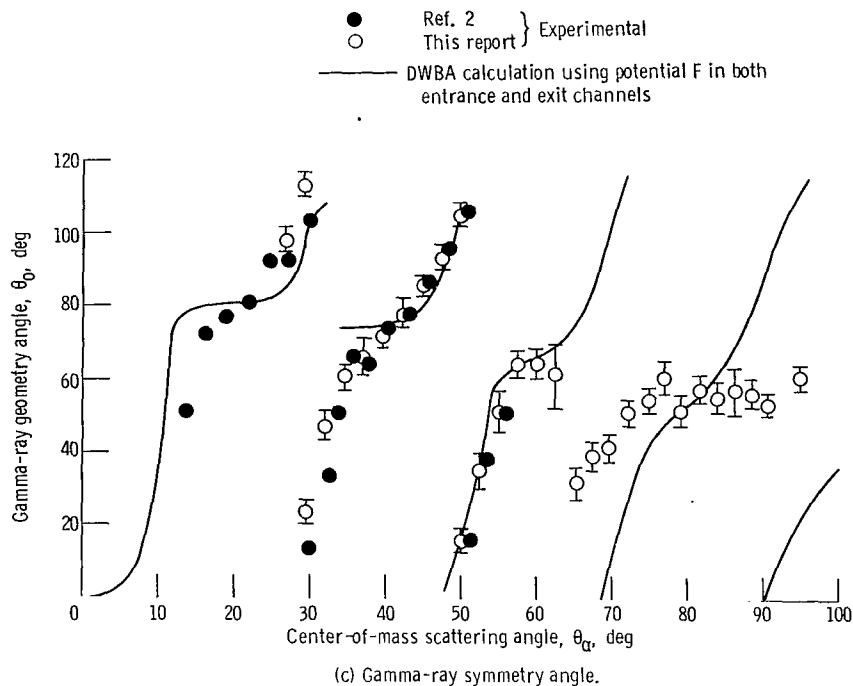
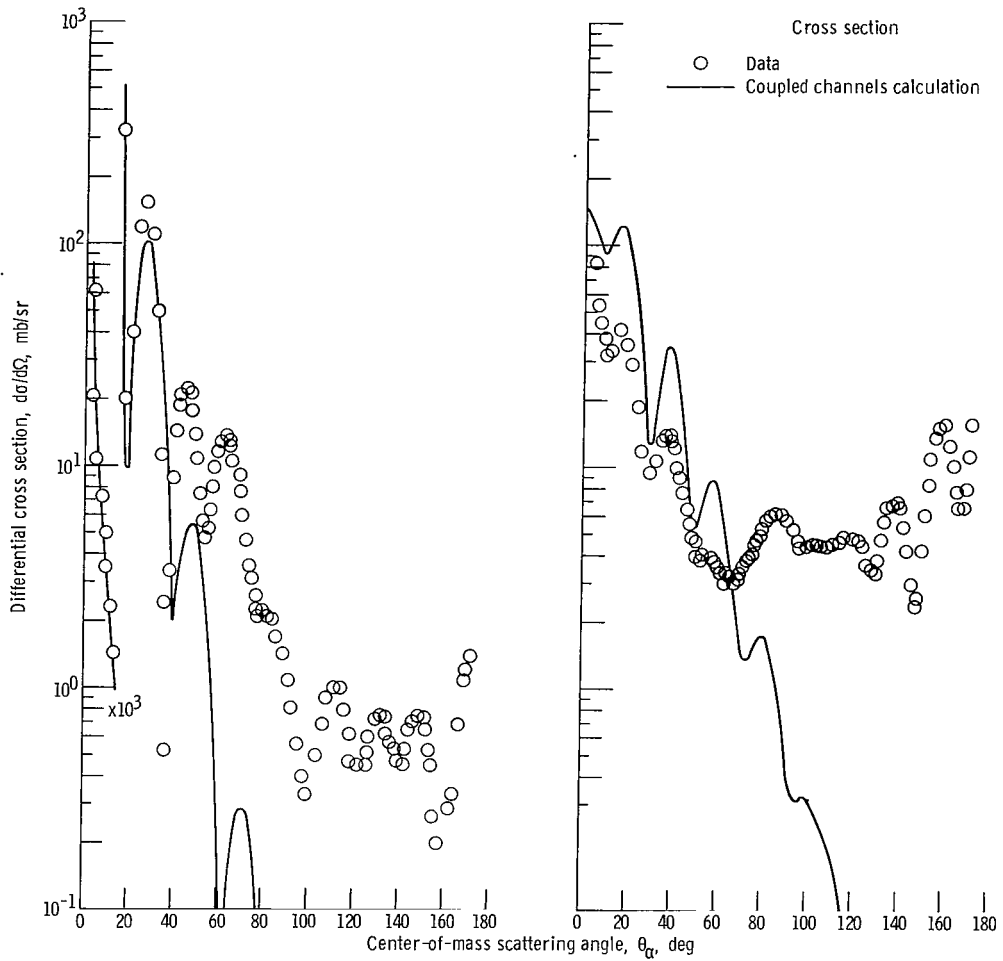


Figure 11. - Concluded.

about 20 MeV which corresponds to an energy of 35.5 MeV as seen by the recoiling carbon nucleus. Data for the elastic scattering of 35.5-MeV alpha particles are available (ref. 12) so attempts were made to find an optical potential which describes these data. The potential which resulted was  $V = 85.96$  MeV,  $W = 13.3$  MeV,  $a_0 = 0.421$  F,  $R_0 = 1.695$  F. The results which were obtained when this potential was used in the exit channel of the DWBA calculation are shown by the dashed lines in parts (b) and (c) of figures 8 to 11. It is clear that no very great changes are made and that in some cases (e.g., the correlation pattern as predicted by potential B) the results are definitely inferior.

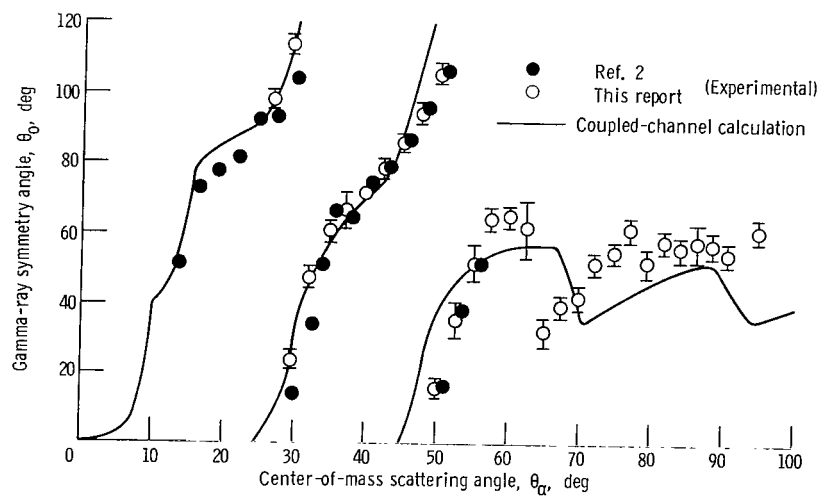
## Coupled-Channel Calculations

One possible reason for the failure of the DWBA calculation to fit the observed data is the fact that it treats the inelastic scattering as a perturbation, with the optical model parameters being determined entirely by the elastic scattering. Examination of the magnitudes of the scattering cross sections will indicate that this is a rather poor approximation since the elastic cross section is a factor of 10 smaller than the inelastic at back angles. It seems logical then to attempt to fit the data using a coupled-channels calculation which treats the elastic and inelastic scattering on an equal basis. The



(a) Elastic scattering.

(b) Inelastic scattering to 4.433-MeV state of carbon-12.



(c) Gamma-ray symmetry angle.

Figure 12. - Cross section for scattering of 41.2-MeV alpha particles from carbon-12. Coupled-channels calculation with  $V = 24.0 \text{ MeV}$ ;  $W = 9.0 \text{ MeV}$ ;  $r_0 = 1.7 \text{ fm}$ ;  $a_0 = 0.50 \text{ fm}$ ; and  $\beta = 0.65$ .

available coupled-channels computer program, unfortunately, requires that the excited nuclear states be described as either rotational or harmonic oscillator states. It is well known that such descriptions are not adequate for carbon-12, so that coupled-channels calculations were not vigorously pursued. For the few calculations which were performed, the EOM program of Wills (ref. 13) was used, with the 4.43- and 7.65-MeV excited states of carbon being described as vibrational states of spin  $2^+$  and  $0^+$ , respectively. Initial calculations were carried out coupling the ground state ( $0^+$ ), the 4.433-MeV ( $2^+$ ), and the 7.65-MeV ( $0^+$ ) state. These proved to be rather time consuming, so that further calculations were done involving only the ground and first excited states, with the intention that any promising results would then be used as a starting point for calculations which coupled three states. Unfortunately, no results were ever found that

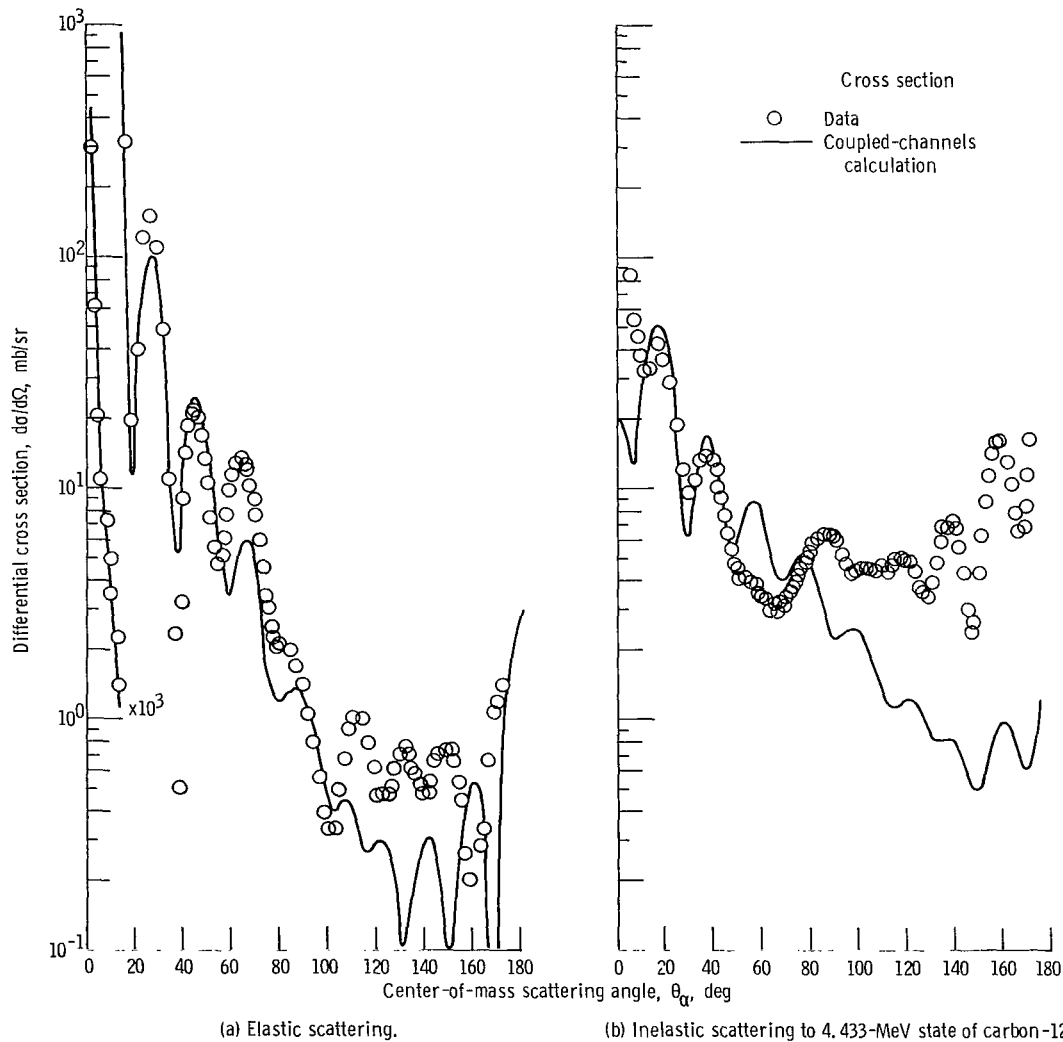


Figure 13. - Cross section for scattering of 41.2-MeV alpha particles from carbon-12. Coupled-channels calculation with  $V = 37.0$  MeV;  $W = 9.0$  MeV;  $r_0 = 1.75$  fm;  $a_0 = 0.45$  fm; and  $\beta = 0.40$ .

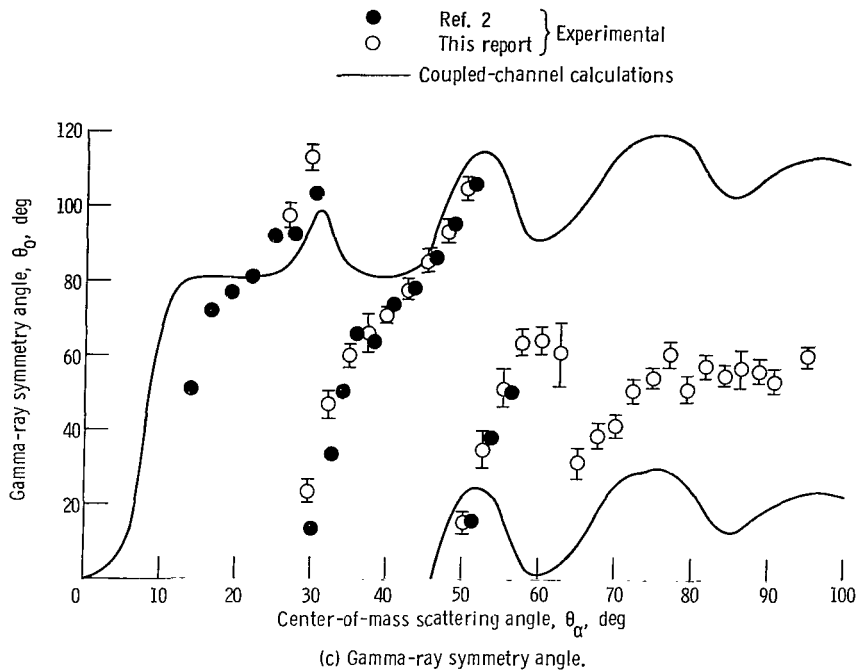


Figure 13. - Concluded.

could be considered promising. In fact no great improvement could be made over the simpler DWBA calculation. Although a reasonable fit could be obtained to the correlation data (as shown in fig. 12), it was only at the expense of the quality of the fit to the cross section data. Attempts to improve the fit to the cross section data were invariably injurious to the correlation fit. In general, it appeared that a real well depth near 24 MeV (as suggested by McDaniels in ref. 1) gave the best fits to the correlation data, but very poor fits to the cross section data, particularly at back angles. A potential depth of about 37 MeV, however, as was needed to represent the back angle cross-section data gave extremely poor correlation predictions. This is shown in figure 13. The other parameters used in these coupled-channels calculations are listed on figures 12 and 13.

## DISCUSSION

### Experimental

The cross section data obtained here are in reasonable agreement with those which have previously been obtained, although the maximum in the 4.433-MeV inelastic scattering observed near  $55^\circ$  by Naqib (ref. 14) is not so pronounced as he reported. This

difference may be attributable to the small difference in incident alpha energy between Naqib's data (42 MeV) and those reported here (41.2 MeV). At back angles the data are reasonably similar to those of Yavin and Farwell (ref. 15).

Angular correlation data, likewise are similar to those of McDaniels (ref. 1) at forward angles where they overlap. At back angles, however, beyond the range studied by Hendrie, it appears that the rapid reverse rotations cease to occur, being replaced by slower oscillations about the adiabatic prediction.

## Possible Reasons for Failure of Theory

The agreement between theory and experiment is generally poor for the elastic and inelastic angular distributions as well as the angular correlation. While it is possible to obtain reasonably good fits to the elastic scattering at angles below approximately  $60^\circ$ , the inelastic distribution in this range cannot be predicted with any great accuracy. In some instances (figs. 8 and 12), it was found that the predicted symmetry angles showed the proper rapid rotation at angles below  $60^\circ$  or  $70^\circ$ , however, at larger angles the agreement was poor in all cases. All the calculations reported here are carried out using a description of the target nucleus which is based on a macroscopic collective model and a description of the scattering in terms of an optical potential. It seems probable that one of these two assumptions is more likely responsible for the failure of the theory to fit all of the data simultaneously.

It is well known that the macroscopic model is inadequate for nuclear structure calculations. The calculation of detailed properties of the nucleus such as energy levels, quadrupole moments, and E2 transition rates requires microscopic descriptions. Detailed calculations of the structure of carbon-12 have been made using Hartree-Fock wave functions, and the results (ref. 16) compare favorably with experiment. Some preliminary calculations of alpha-particle scattering cross sections for carbon-12 and magnesium-24 have been made in which microscopic wave functions were used, however, it was found that the use of these wave functions does not improve the overall result (ref. 17).

One is led then to question whether the use of the optical model is realistic. Since the optical model is basically statistical, it should not be surprising to find it difficult to predict the elastic and inelastic cross sections for a system with only 12 particles. However, if we wish to obtain sufficient information to determine whether the optical model is at fault, then a much more detailed calculation is required (ref. 18). Essentially, one must calculate the scattering wave functions by using an effective potential which is computed in terms of the projectile-target interaction and the target wave function. For the case of interest here ( $^{12}\text{C}$ ), there are sufficiently few nucleons involved that a realistic calculation could be done. The alpha-particle model of carbon-12 has

met with some success in structure calculations (ref. 19), and wave functions obtained from such a model are compatible with the type of calculation suggested. Furthermore, the use of such a wave function would make it a simple matter to examine exchange effects that may be important if the alpha-cluster model is a good representation for carbon-12. The projectile-nucleus interaction may be replaced by a sum of alpha-alpha interactions, and the effective potential calculated in terms of these. If an approach of this type does not improve the results significantly then the reaction mechanism must be questioned for the light nuclei.

Lewis Research Center,  
National Aeronautics and Space Administration,  
Cleveland, Ohio, August 26, 1969,  
129-02.

## REFERENCES

1. McDaniels, D. K.; Hendrie, D. L.; Bassel, R. H.; and Satchler, G. R.: Alpha-Gamma Angular Correlations and the Distorted-Waves Theory. *Phys. Letters*, vol. 1, no. 7, July 1, 1962, pp. 295-297.
2. Hendrie, David L.: A Study of Coincidences Between Inelastically Scattered 42-MeV Alpha Particles and De-excitation Gamma Rays. Ph.D. Thesis, Univ. Washington, 1964.
3. Eidson, W. W.; Cramer, J. G., Jr.; Blatchley, D. E.; and Bent, R. D.: Angular Correlation Studies of Nuclear Polarization Following Inelastic Scattering of Alpha Particles from  $C^{12}$  and  $Mg^{24}$ . *Nucl. Phys.*, vol. 55, 1964, pp. 613-642.
4. Blair, J. S.; and Wilets, L.: Gamma-Ray Correlation Function in the Adiabatic Approximation. *Phys. Rev.*, vol. 121, no. 5, Mar. 1, 1961, pp. 1493-1499.
5. Satchler, G. R.: Gamma Radiation Following the Surface Scattering of Nucleons. *Proc. Phys. Soc. (London)*, Sec. A, vol. 68, pt. 11, Nov. 1955, pp. 1037-1040.
6. Wills, J. G.; and Cramer, J. G., Jr.: Angular Momentum Selection and Angular Correlations in Direct Reactions with Strongly Absorbed Particles. *Nuclear Spectroscopy with Direct Reactions. I. Contributed Papers.* F. E. Throw, ed. Rep. ANL-6848, Argonne National Lab., Mar. 1964, pp. 147-152.
7. Inglis, D. R.: Reverse Rotation of Gamma-Ray Angular Pattern with Changing Alpha-Scattering Angle. *Phys. Letters*, vol. 10, no. 3, June 15, 1964, pp. 336-338.

8. Leonard, Regis F.; Stewart, William M.; Baron, Norton; Braley, Richard C.:  
Gamma Ray Angular Correlations Following Inelastic Scattering of 42-MeV Alpha  
Particles from Magnesium 24. NASA TN D-4683, 1968.
9. Leonard, Regis F.; Stewart, William M.; and Baron, Norton: Elastic and Inelas-  
tic Scattering of 42-MeV Alpha Particles from Even Tellurium Isotopes. NASA  
TN D-3991, 1967.
10. Melkanoff, Michel A.; Nodvik, John S.; Saxon, David S.; and Cantor, David G.:  
A FORTRAN Program for Elastic Scattering Analyses with the Nuclear Optical  
Model. University of California Press, 1961.
11. Gibbs, W. R.; Madsen, V. A.; Miller, J. A.; Tobocman, W.; Cox, E. C.; and  
Mowry, L.: Direct Reaction Calculation. NASA TN D-2170, 1964.
12. Mikumo, Takashi: Anomalies in the Scattering of Alpha Particles by Carbon. J.  
Phys. Soc. Japan, vol. 16, no. 6, June 1961, pp. 1066-1076.
13. Wills, John G.: An Extended Optical Model. Ph.D. Thesis, Univ. Washington,  
1963.
14. Naqib, Isam M.: Excitation of Nuclear Levels in  $Mg^{24}$ ,  $Al^{27}$ , and  $C^{12}$  Through In-  
elastic Scattering of Alpha Particles. Ph.D. Thesis, Univ. Washington, 1962.
15. Yavin, A. I.; and Farwell, G. W.: Angular Distributions for Elastic and Inelastic  
Scattering of 40-MeV Alpha Particles by Carbon, Nitrogen, Oxygen, and Argon.  
Nucl. Phys., vol. 12, 1959, pp. 1-34.
16. Bouten, M.; Van Leuven, P.; and Depuydt, H.: A Projected Hartree-Fock Calcula-  
tion for  $^{12}C$ . Nucl. Phys., vol. A94, 1967, pp. 687-697.
17. Braley, R. C.; and Ford, W. F.: Inelastic Scattering Calculations Using Projected  
Hartree-Fock Wave Functions. Phys. Rev., vol. 182, no. 4, June 20, 1969,  
pp. 1174-1185.
18. Schenter, R. E.: Extreme Damping of the Single-Particle Wave Functions in the  
Nuclear Interior. Phys. Rev. Letters, vol. 18, no. 12, Mar. 20, 1967.
19. Brink, D.: The Alpha-Particle Model of Light Nuclei. Many-Body Description of  
Nuclear Structure and Reactions. Course XXXVI of Proceedings of the Interna-  
tional School of Physics "Enrico Fermi." C. Bloch, ed., Academic Press,  
1966, pp. 247-277.

TABLE I. - DIFFERENTIAL CROSS SECTIONS AND STATISTICAL ERRORS  
FOR SCATTERING OF 42-MeV ALPHA PARTICLES BY CARBON-12

(a) Elastic scattering

Center-of-mass scattering angle, $\theta_{cm}$ , deg	Differential cross section, $d\sigma/d\Omega$ , mb/sr	Center-of-mass scattering angle, $\theta_{cm}$ , deg	Differential cross section, $d\sigma/d\Omega$ , mb/sr	Center-of-mass scattering angle, $\theta_{cm}$ , deg	Differential cross section, $d\sigma/d\Omega$ , mb/sr
2.84	311 060±1330	57.56	7.84±0.03	115.54	0.784±0.010
4.17	63 330±300	58.81	9.83±0.12	117.46	.597±0.008
5.50	21 110±100	60.05	11.5±0.1	119.35	.450±0.008
6.84	10 880±70	61.29	12.9±0.1	121.21	.441±0.008
8.17	7 230±40	62.52	13.3±0.1	123.05	.437±0.008
9.50	4 980±30	63.75	13.4±0.1	124.87	.503±0.008
10.83	3 540±20	64.97	12.7±0.1	126.67	.586±0.090
12.16	2 240±20	66.19	12.0±0.1	128.44	.693±0.001
13.49	1 400±10	67.40	10.2±0.1	130.18	.740±0.011
16.15	332.2±4.1	68.62	8.98±0.12	131.91	.691±0.010
18.80	14.9±0.5	69.83	7.43±0.03	133.62	.595±0.010
21.48	40.9±0.9	71.03	5.86±0.09	135.30	.546±0.010
24.09	125.3±0.3	72.22	4.53±0.02	136.96	.508±0.010
26.72	149.7±0.1	73.41	3.40±0.07	138.60	.462±0.009
29.35	111.7±0.2	74.60	2.99±0.02	140.22	.457±0.009
31.97	50.3±0.1	75.78	2.49±0.06	141.83	.520±0.010
34.58	10.8±0.1	76.96	2.20±0.02	143.41	.635±0.012
35.88	2.36±0.03	78.13	1.99±0.06	144.97	.686±0.012
37.18	0.502±0.012	79.30	2.13±0.01	146.52	.704±0.014
38.48	3.17±0.06	81.62	2.04±0.01	148.05	.732±0.020
39.77	8.77±0.05	83.91	1.95±0.01	149.57	.710±0.015
41.06	14.2±0.1	86.18	1.66±0.01	151.07	.643±0.019
42.35	18.8±0.1	88.44	1.39±0.01	152.55	.509±0.014
43.64	21.7±0.2	90.67	1.06±0.01	154.02	.430±0.022
44.92	22.0±0.1	92.87	0.785±0.009	155.48	.248±0.010
46.20	20.4±0.1	95.05	.544±0.008	156.92	.193±0.026
47.48	17.1±0.1	97.21	.383±0.006	158.35	0.0772±0.0233
48.75	13.7±0.1	99.35	.315±0.006	162.58	.272±0.010
50.02	10.6±0.1	101.46	.321±0.006	163.97	.324±0.024
51.28	7.37±0.07	103.54	.475±0.007	165.35	.638±0.015
52.55	5.48±0.03	105.60	.646±0.008	168.09	1.03±0.02
53.81	4.61±0.08	107.64	.890±0.010	169.45	1.15±0.02
55.07	5.11±0.03	109.65	.988±0.010	170.80	1.38±0.02
56.32	6.18±0.09	113.60	.983±0.010		

TABLE I. - Continued. DIFFERENTIAL CROSS SECTIONS AND STATISTICAL  
 ERRORS FOR SCATTERING OF 42-MeV ALPHA PARTICLES BY CARBON-12

(b) Inelastic scattering to 4.433-MeV state of carbon-12

Center-of- mass scattering angle, $\theta_{cm}$ deg	Differential cross section, $d\sigma/d\Omega$ , mb/sr	Center-of- mass scattering angle, $\theta_{cm}$ deg	Differential cross section, $d\sigma/d\Omega$ , mb/sr	Center-of- mass scattering angle, $\theta_{cm}$ deg	Differential cross section, $d\sigma/d\Omega$ , mb/sr
5.61	88.45±6.45	63.69	3.022±0.017	120.94	4.829±0.026
6.91	56.64±4.86	64.94	3.149±0.066	122.79	4.436±0.025
8.33	47.85±3.15	66.18	3.072±0.021	124.62	3.740±0.024
9.69	39.71±2.89	67.42	3.224±0.067	126.42	3.566±0.023
11.04	33.32±1.78	68.65	3.174±0.017	128.20	3.454±0.023
13.76	34.71±1.41	69.88	3.495±0.071	129.95	3.902±0.026
16.46	43.54±2.81	71.11	3.615±0.018	131.68	4.869±0.030
19.17	37.54±0.86	72.33	3.792±0.075	133.38	5.976±0.032
21.87	30.13±0.75	73.54	3.901±0.020	135.06	6.825±0.036
24.56	19.29±0.134	74.75	4.282±0.080	136.71	6.919±0.038
27.24	12.19±0.035	75.95	4.550±0.020	138.34	7.447±0.039
29.92	9.779±0.052	77.15	4.887±0.086	139.95	6.762±0.038
32.59	11.06±0.055	78.34	5.074±0.023	141.54	5.616±0.035
35.25	13.59±0.064	79.53	5.484±0.093	143.11	4.359±0.031
36.58	14.19±0.060	80.71	5.942±0.024	144.66	3.027±0.029
37.90	14.05±0.062	83.06	6.283±0.024	146.18	2.435±0.025
39.22	13.56±0.131	85.38	6.553±0.026	147.69	2.679±0.028
40.54	12.36±0.062	87.67	6.284±0.025	149.18	4.313±0.047
41.87	10.18±0.067	89.95	5.871±0.023	150.66	6.369±0.042
43.17	9.292±0.055	92.20	5.257±0.023	152.11	8.949±0.066
44.48	7.810±0.101	94.42	4.713±0.021	153.55	11.56±0.059
45.79	6.511±0.042	96.62	4.412±0.022	154.98	14.41±0.089
47.09	5.614±0.062	98.79	4.471±0.021	156.39	16.20±0.062
48.39	4.820±0.034	100.94	4.574±0.021	157.78	16.23±0.103
49.68	4.627±0.079	103.06	4.528±0.022	159.17	16.73±0.075
50.98	4.153±0.026	105.16	4.565±0.022	161.90	13.09±0.071
52.27	4.173±0.055	107.22	4.497±0.022	163.25	10.52±0.052
53.55	4.000±0.022	109.26	4.545±0.022	164.59	8.026±0.059
54.84	3.973±0.074	111.28	4.505±0.022	165.92	6.693±0.044
56.11	3.925±0.024	113.26	4.760±0.023	167.24	6.834±0.046
57.39	3.827±0.073	115.22	5.024±0.024	168.56	8.542±0.051
58.66	3.543±0.021	117.16	5.101±0.026	169.87	11.68±0.061
59.92	3.581±0.070	119.06	5.036±0.025	171.17	16.77±0.073
61.18	3.328±0.022				
62.44	3.385±0.068				

TABLE I. - Continued. DIFFERENTIAL CROSS SECTIONS AND STATISTICAL  
EFFORS FOR SCATTERING OF 42-MeV ALPHA PARTICLES BY CARBON-12

(c) Inelastic scattering to 7.65-MeV state of carbon-12

Center-of- mass scattering angle, $\theta_{cm}$ , deg	Differential cross section, $d\sigma/d\Omega$ , mb/sr	Center-of- mass scattering angle, $\theta_{cm}$ , deg	Differential cross section, $d\sigma/d\Omega$ , mb/sr	Center-of- mass scattering angle, $\theta_{cm}$ , deg	Differential cross section, $d\sigma/d\Omega$ , mb/sr
19.50	3.121±0.056	66.02	0.478±0.026	116.69	0.526±0.010
22.25	2.247±0.044	67.28	.580±0.009	118.62	.783±0.011
24.98	.768±0.030	68.53	.704±0.031	120.52	.523±0.011
27.72	.143±0.006	69.78	.799±0.009	122.39	.579±0.012
30.44	.588±0.014	71.03	.887±0.036	124.26	.826±0.013
33.16	1.547±0.022	72.27	.900±0.009	126.04	.704±0.012
35.33	2.113±0.027	73.50	.958±0.037	127.77	.467±0.012
37.21	2.207±0.024	74.73	.751±0.009	129.63	.209±0.009
38.56	1.836±0.024	75.96	.702±0.032	131.31	.150±0.008
39.90	1.685±0.046	77.17	.637±0.008	132.97	.339±0.011
41.24	1.107±0.020	78.39	.562±0.029	134.65	.219±0.011
42.58	.688±0.022	79.59	.520±0.008	136.33	.140±0.011
43.91	.375±0.011	80.79	.488±0.027	138.00	.507±0.015
45.24	.204±0.016	81.99	.535±0.007	139.57	.618±0.016
46.57	.142±0.007	84.36	.526±0.007	141.12	.519±0.016
47.89	.246±0.013	86.71	.546±0.008	142.71	.358±0.015
49.21	.415±0.010	89.03	.444±0.007	144.25	.203±0.015
50.53	.578±0.027	91.32	.259±0.005	145.77	.350±0.018
51.84	.844±0.011	93.59	.110±0.004	147.24	.176±0.016
53.15	1.047±0.028	95.83	0.0292±0.0025	148.75	.309±0.018
54.46	1.025±0.012	98.04	.0476±0.0030	150.18	.268±0.026
55.76	.945±0.036	100.23	.132±0.004	151.66	.719±0.024
57.06	.889±0.012	102.39	.207±0.005	153.09	.888±0.033
58.35	.801±0.033	104.52	.231±0.005	154.44	1.249±0.033
59.64	.529±0.008	106.62	.182±0.005	155.83	1.362±0.049
60.92	.492±0.026	108.69	.110±0.005	157.21	1.376±0.029
62.20	.339±0.008	110.74	.0116±0.0026	158.56	1.574±0.072
63.48	.323±0.021	112.75	.0227±0.0030	159.91	.950±0.045
64.75	.358±0.007	114.74	.0964±0.0053		

TABLE I. - Concluded. DIFFERENTIAL CROSS SECTIONS AND STATISTICAL ERRORS FOR SCATTERING OF 42-MeV ALPHA PARTICLES BY CARBON-12

(d) Inelastic scattering to 9.61-MeV state of carbon-12

Center-of-mass scattering angle, $\theta_{cm}$ , deg	Differential cross section, $d\sigma/d\Omega$ , mb/sr	Center-of-mass scattering angle, $\theta_{cm}$ , deg	Differential cross section, $d\sigma/d\Omega$ , mb/sr	Center-of-mass scattering angle, $\theta_{cm}$ , deg	Differential cross section, $d\sigma/d\Omega$ , mb/sr
19.74	10.09±0.11	59.05	1.90±0.05	94.60	0.847±0.011
22.52	8.69±0.10	60.36	2.18±0.02	96.86	.984±0.012
25.29	7.14±0.10	61.65	1.96±0.05	99.08	1.10±0.02
28.06	4.78±0.03	62.95	1.98±0.02	101.28	1.14±0.02
30.82	3.72±0.03	64.24	2.10±0.05	103.45	1.68±0.02
33.56	3.25±0.04	65.52	1.52±0.03	105.58	1.52±0.02
36.30	3.62±0.05	66.80	1.35±0.04	107.69	1.19±0.02
37.67	4.03±0.04	68.07	1.26±0.02	109.77	.904±0.015
39.03	3.90±0.04	69.34	0.969±0.036	111.81	1.36±0.02
40.39	5.01±0.09	70.60	.680±0.011	113.83	1.29±0.02
41.74	4.54±0.05	71.86	.627±0.031	115.81	1.22±0.02
43.10	4.34±0.05	73.11	.517±0.010	117.77	1.62±0.02
44.45	4.28±0.03	74.36	.640±0.030	119.69	1.55±0.02
45.79	4.33±0.08	75.60	.637±0.012	121.58	1.71±0.02
47.14	3.75±0.04	76.84	.788±0.034	123.45	1.82±0.02
48.48	3.41±0.04	78.06	.979±0.013	125.29	1.78±0.02
49.81	2.87±0.04	79.29	1.13±0.04	127.08	1.10±0.02
51.14	2.02±0.05	80.50	1.10±0.02	128.83	1.27±0.02
52.47	2.35±0.02	82.92	1.42±0.02	130.59	.992±0.019
53.80	2.12±0.03	85.31	1.36±0.02	132.28	.793±0.019
55.12	1.99±0.02	87.67	1.17±0.02	134.00	1.29±0.02
56.43	1.91±0.05	90.01	0.961±0.012	135.64	1.35±0.03
57.74	2.14±0.02	92.32	.916±0.011	137.26	1.39±0.03

TABLE II. - EXPERIMENTAL RESULTS OF

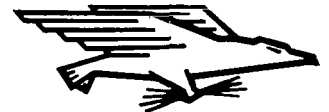
CARBON-12 ( $\alpha$ ,  $\alpha'\gamma$  4.433 MeV)

Scattering angle for alpha par- ticles in center- of-mass system, $\theta_{\alpha}$	Symmetry angle of alpha-gamma correlation func- tion, $\theta_0$	Ratio of iso- tropic to anisotropic component, A/B
26.55	7.81±2.43	0.13±0.068
31.80	47.06±2.42	.25±0.074
37.01	66.27±5.33	0±0.03
42.18	78.60±2.17	0.024±0.058
47.31	3.38±1.72	0±0.03
52.38	35.02±5.20	.314±0.179
57.40	63.86±3.40	.097±0.098
62.35	61.21±7.90	1.95±1.15
67.24	38.99±2.34	.079±0.069
72.05	51.16±1.21	.061±0.035
76.79	60.75±2.86	.083±0.081
81.45	57.25±2.89	.238±0.093
86.01	57.23±5.44	.413±0.218
29.18	23.60±1.90	.264±0.066
34.41	60.47±1.74	.121±0.051
39.60	71.53±1.02	0±0.03
44.75	85.71±1.60	0±0.03
49.85	15.20±1.87	.128±0.055
54.90	51.48±4.48	.220±0.135
59.88	64.12±3.30	.352±0.125
64.80	31.97±3.48	.409±0.139
69.66	41.57±2.42	.139±0.067
74.43	54.52±1.84	.125±0.050
79.13	51.57±3.01	.601±0.144
83.74	55.47±2.17	.338±0.077
88.27	56.56±2.56	.093±0.072
90.50	53.69±1.14	.059±0.032
94.88	60.73±1.27	0±0.03

TABLE III. - RESULTS OF OPTICAL MODEL CALCULATIONS FOR 41-MeV ALPHA  
PARTICLES SCATTERED BY NICKEL-58

Potential	Real strength, V, MeV	Imaginary strength, W, MeV	Diffuseness of real potential, $a_0$ , fm	Diffuseness of imaginary potential, $a_1$ , fm	Radius of real potential, $r_0$ , fm	Radius of imaginary potential, $r_1$ , fm	Goodness of fit per data point, $\chi^2/N$
A	24.0	13.0	0.420	-----	1.99	-----	48.8
B	37.16	13.27	.452	-----	1.846	-----	20.6
C	37.11	13.26	.451	-----	1.846	-----	20.6
D	82.73	15.03	.377	-----	1.767	-----	23.4
E	199.1	42.17	.650	-----	1.262	-----	-----
F	31.46	15.78	.375	0.246	2.00	1.926	19.8

FIRST CLASS MAIL



POSTAGE AND FEES PAID  
NATIONAL AERONAUTICS AND  
SPACE ADMINISTRATION

CGU OGI 49 51 3DS 69321 00903  
AIR FORCE WEAPONS LABORATORY/WLIL/  
KIRTLAND AIR FORCE BASE, NEW MEXICO 8711

ATTN: F. LOU BULMAN, CHIEF, TECH. LIBRARY

POSTMASTER: If Undeliverable (Section 158  
Postal Manual) Do Not Return

*"The aeronautical and space activities of the United States shall be conducted so as to contribute . . . to the expansion of human knowledge of phenomena in the atmosphere and space. The Administration shall provide for the widest practicable and appropriate dissemination of information concerning its activities and the results thereof."*

— NATIONAL AERONAUTICS AND SPACE ACT OF 1958

## NASA SCIENTIFIC AND TECHNICAL PUBLICATIONS

**TECHNICAL REPORTS:** Scientific and technical information considered important, complete, and a lasting contribution to existing knowledge.

**TECHNICAL NOTES:** Information less broad in scope but nevertheless of importance as a contribution to existing knowledge.

**TECHNICAL MEMORANDUMS:** Information receiving limited distribution because of preliminary data, security classification, or other reasons.

**CONTRACTOR REPORTS:** Scientific and technical information generated under a NASA contract or grant and considered an important contribution to existing knowledge.

**TECHNICAL TRANSLATIONS:** Information published in a foreign language considered to merit NASA distribution in English.

**SPECIAL PUBLICATIONS:** Information derived from or of value to NASA activities. Publications include conference proceedings, monographs, data compilations, handbooks, sourcebooks, and special bibliographies.

**TECHNOLOGY UTILIZATION PUBLICATIONS:** Information on technology used by NASA that may be of particular interest in commercial and other non-aerospace applications. Publications include Tech Briefs, Technology Utilization Reports and Notes, and Technology Surveys.

*Details on the availability of these publications may be obtained from:*

SCIENTIFIC AND TECHNICAL INFORMATION DIVISION  
NATIONAL AERONAUTICS AND SPACE ADMINISTRATION  
Washington, D.C. 20546